JOC The Journal of Organic Chemistry
Cite This: J. Org. Chem. 2019, 84, 1534−1541
Article
pubs.acs.org/joc

Emeridones A−F, a Series of 3,5-Demethylorsellinic Acid-Based Meroterpenoids with Rearranged Skeletons from an Endophytic Fungus *Emericella* sp. TJ29

Qin Li,[†,∥] Chunmei Chen,[†,∥] Li Cheng,[†,‡] Mengsha Wei,[†] Chong Dai,[†] Yan He,[§] Jiaojiao Gong,[†] Runqi Zhu,[†] Xiao-Nian Li,[⊥] Junjun Liu,[†] Jianping Wang,[†] Hucheng Zhu,*[,†] and Yonghui Zhang*[,†]

[†]Hubei Key Laboratory of Natural Medicinal Chemistry and Resource Evaluation, School of Pharmacy, Tongji Medical College and [§]Tongji Hospital, Tongji Medical College, Huazhong University of Science and Technology, Wuhan 430030, China

[‡]College of Pharmacy, Hubei University of Medicine, Shiyan 442000, China

[⊥]State Key Laboratory of Phytochemistry and Plant Resources in West China, Kunming Institute of Botany, Chinese Academy of Sciences, Kunming 650201, China

Supporting Information

ABSTRACT: Six new 3,5-demethylorsellinic acid-based meroterpenoids, emeridones A−F (**1**−**6**), and eight known analogues (**7**−**14**) were isolated from *Emericella* sp. TJ29. Their structures and absolute configurations were elucidated by comprehensive spectroscopic analyses, single-crystal X-ray diffraction experiments, and electronic circular dichroism calculations. Emeridone A (**1**) represents the first meroterpenoid featuring a unique rigid 6/6/5/6 tetracyclic carbon ring system with two additional lactone rings. Emeridones B and C (**2** and **3**) possess a 2,6-dioxabicyclo[2.2.1]heptane and a spiro[bicyclo[3.2.2]nonane-2,1′-cyclohexane] moiety, respectively, and both functionalities were found for the second time in meroterpenoids. These new compounds were evaluated for their cytotoxic activities against five human cancer cells, and compounds **2**, **4**, and **6** exhibited moderate cytotoxic activities, with IC_{50} values ranging from 8.19 to 18.80 μM.

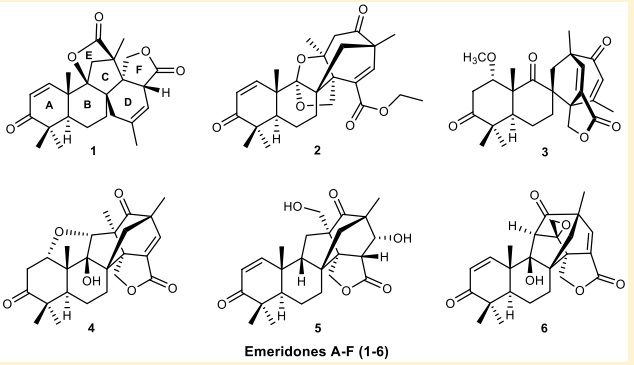

INTRODUCTION

Meroterpenoids have received considerable attention from both chemists and pharmacologists because of their intriguing structures and potent biological functions, such as anti-inflammatory,[1] cytotoxic,[2] and antimicrobial activities.[3] 3,5-Demethylorsellinic acid-based meroterpenoids normally possess complex skeletons, and studies on this type of meroterpenoid have achieved unprecedented progress in their structural exploration and biosynthesis.[4−6] In our previous research, a series of new 3,5-demethylorsellinic acid-based meroterpenoids have been discovered from *Aspergillus terreus* of various origins and an endophytic fungus *Emericella* sp. TJ29.[7,8] Because the secondary metabolites of fungi will be significantly affected by the culture condition,[9] in this study, we preliminarily investigated the secondary metabolites of the fungus *Emericella* sp. TJ29 cultured in a liquid broth, which led to the isolation of six new and eight known 3,5-demethylorsellinic acid-based meroterpenoids (Figure 1). Emeridone A (**1**) represents the first 3,5-demethylorsellinic acid-based meroterpenoid featuring a unique rigid 6/6/5/6 tetracyclic carbon ring system with two additional lactone rings. Emeridones B and C (**2** and **3**) possess a 2,6-dioxabicyclo[2.2.1]heptane and a spiro[bicyclo[3.2.2]-nonane-2,1′-cyclohexane] functionality, sharing the same skeletons as our previously reported compounds aspermerodione and spiroaspertrione A, respectively.[10,11] Herein the isolation, structural elucidation, and plausible biosynthetic pathway of **1** as well as the bioactivity evaluations of these new compounds are presented.

RESULTS AND DISCUSSION

Emeridone A (**1**) was initially isolated as a colorless amorphous powder. The molecular formula of $C_{25}H_{30}O_5$, with 11 degrees of unsaturation, was established by the presence of an $[M + Na]^+$ ion peak at m/z 433.2002 in the HRESIMS spectrum, in combination with the ^{13}C NMR data. The ^1H NMR spectroscopic data (Table 1), together with the HSQC spectra of **1**, suggested the presence of three olefinic protons at δ_H 7.02 (d, J = 10.1 Hz, H-1), 5.91 (d, J = 10.1 Hz, H-2), and 5.38 (br s, H-6′), an oxygenated methylene at δ_H 4.09 (d, J = 9.7 Hz, H-1′) and 4.06 (d, J = 9.7 Hz, H-1′), and five methyl groups at δ_H 1.82 (s, H3−10′), 1.41 (s, H_3-13), 1.21 (s, H_3-9′), 1.17 (s, H_3-14), and 1.11 (s, H_3-15). The ^{13}C NMR and DEPT spectra (Table 2) of **1** displayed 25 carbon resonances, including a ketone

Received: November 21, 2018
Published: January 4, 2019

DOI: 10.1021/acs.joc.8b02830
J. Org. Chem. 2019, 84, 1534−1541

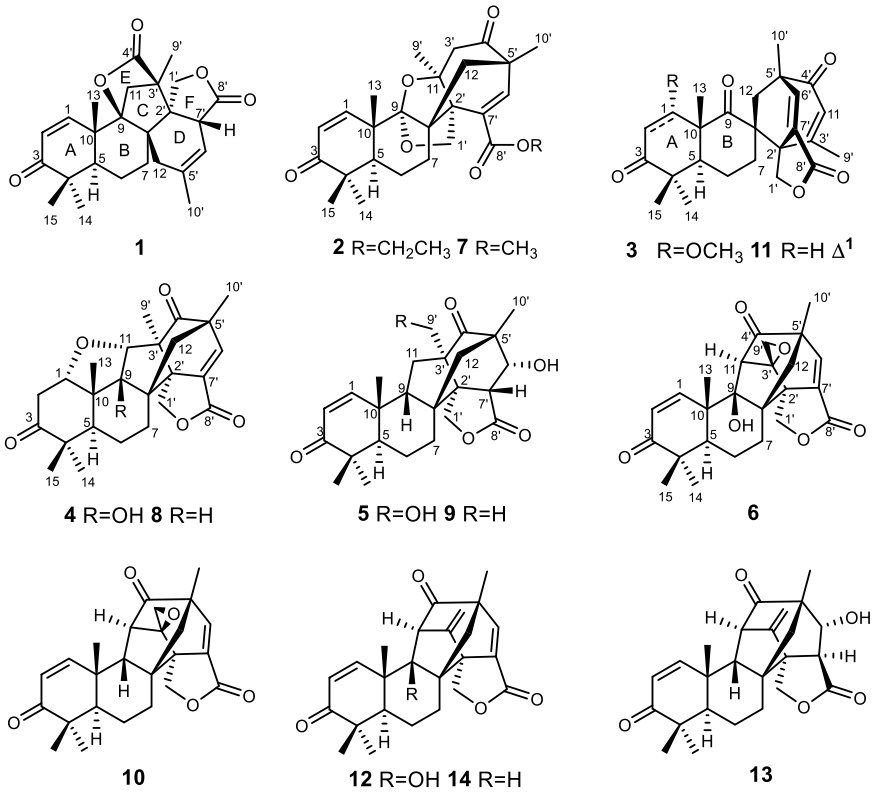

Figure 1. Structures of compounds **1**−**14**.

Table 1. ^{1}H (400 MHz) NMR Data of Compounds 1−6 (δ in ppm, J in Hz)

no.	1[a]	2[a]	3[a]	4[a]	5[a]	6[b]
1	7.02 d (10.1)	7.31 d (10.1)	3.95 t (3.3)	3.81 t (6.6)	6.33 d (10.1)	6.91 d (10.3)
2	5.91 d (10.1)	5.91 d (10.1)	2.69 t (3.3)	2.81 m	5.85 d (10.1)	5.82 d (10.3)
5	1.82 m	2.37 m	2.37 dd (10.6, 4.3)	1.87 dd (14.2, 4.3)	1.28 m	2.38 dd (13.7, 5.9)
6	1.82 m; 1.67 m	1.64 m	1.77 m	1.68 m; 1.52 m	1.81 m; 1.65 m	1.79 m; 1.65 m
7	1.64 m; 1.17 m	1.65 m; 1.27 m	1.58 m	1.77 m	1.93 m; 1.82 m	2.07 m; 1.90 m
9					1.57 dd (10.6, 8.0)	
11a	2.32 d (11.4)	2.69 d (19.0)	5.74 s	3.45 s	1.78 m	2.90 s
11b	1.84 d (11.4)	2.53 d (19.0)				
12a	2.30 overlap	2.25 d (14.9)	2.01 d (13.3)	2.72 d (12.7)	1.26 overlap	2.44 overlap
12b	2.17 d (15.2)	1.49 d (14.9)	1.91 d (13.3)	1.02 overlap	1.17 d (13.5)	1.33 d (11.9)
13	1.41 s	1.25 s	1.15 s	0.79 s	1.24 s	1.27 s
14	1.17 s	1.16 s	1.14 s	1.05 s	1.09 s	1.20 s
15	1.11 s	1.11 s	1.10 s	1.16 s	1.03 s	1.13 s
1′a	4.09 d (9.7)	4.72 d (9.1)	4.90 d (11.3)	4.98 d (10.1)	4.32 d (9.6)	4.52 d (9.6)
1′b	4.06 d (9.7)	4.06 d (9.1)	4.35 d (11.3)	4.69 d (10.1)	4.05 overlap	4.41 d (9.6)
6′	5.38 br s	6.90 s	6.78 s	7.22 s	4.03 overlap	6.92 s
7′	2.85 m				3.00 d (7.6)	
9′	1.21 s	1.33 s	2.23 s	1.15 s	3.89 d (11.3)	2.72 d (3.5);
					3.71 d (11.3)	2.43 overlap
10′	1.82 s	1.48 s	1.46 s	1.32 s	1.12 s	1.36 s
11′		4.21 q (7.0)	3.28 s			
12′		1.32 t (7.0)				

[a]Recorded in $CDCl_3$. [b]Recorded in CD_3OD.

carbonyl (δ_C 203.1), two ester carboxyl groups (δ_C 176.6 and 176.1), four olefinic carbons (δ_C 153.7, 139.3, 126.2, and 116.0), ten nonprotonated carbons including an oxygenated one (δ_C 92.3), five methines, five methylenes including an oxygenated one (δ_C 70.9), and five methyl groups.

All proton resonances were assigned to their respective carbons via the HSQC spectrum. The planar structure of **1** was elucidated on the basis of ^{1}H−^{1}H COSY and HMBC experiments (Figure 2). Three isolated proton spin systems, H-1/H-2, H-5/H_2-6/H_2-7, and H-6′/H-7′, were disclosed by the ^{1}H−^{1}H COSY spectrum, in addition to the observed HMBC correlations from H-2 to C-4, from H_3-15 to C-3, C-4, C-5, and C-14, from H_2-7 to C-8 and C-9, and from H_3-13 to C-1, C-5, C-9, and C-10 established the structure of rings A and B. The

DOI: 10.1021/acs.joc.8b02830
J. Org. Chem. 2019, 84, 1534−1541

Table 2. ^{13}C (100 MHz) NMR Data of Compounds 1−6

no.	1[a]	2[a]	3[a]	4[a]	5[a]	6[b]
1	153.7, CH	155.7, CH	81.1, CH	83.7, CH	154.0, CH	155.5, CH
2	126.2, CH	126.5, CH	38.5, CH_2	40.1, CH_2	125.8, CH	126.1, CH
3	203.1, C	204.5, C	213.2, C	214.2, C	203.7, C	206.2, C
4	44.2, C	44.6, C	47.0, C	46.9, C	44.2, C	45.7, C
5	47.1, CH	46.8, CH	43.7, CH	40.7, CH	38.8, CH	40.4, CH
6	19.2, CH_2	18.8, CH_2	18.0, CH_2	16.9, CH_2	18.4, CH_2	17.8, CH_2
7	33.9, CH_2	31.2, CH_2	35.0, CH_2	28.4, CH_2	24.1, CH_2	25.6, CH_2
8	50.2, C	53.8, C	60.0, C	51.8, C	45.9, C	52.2, C
9	92.3, C	109.6, C	214.6, C	88.8, C	55.3, CH	85.4, C
10	40.8, C	41.9, C	54.1, C	49.6, C	38.6, C	45.0, C
11	43.4, CH_2	51.6, C	125.0, CH	95.3, CH	34.8, CH_2	73.3, CH
12	35.4, CH_2	38.4, CH_2	44.8, CH_2	46.3, CH_2	51.3, CH_2	48.9, CH_2
13	19.3, CH_3	19.2, CH_3	18.3, CH_3	13.5, CH_3	22.9, CH_3	18.9, CH_3
14	21.7, CH_3	21.5, CH_3	22.1, CH_3	13.6, CH_3	21.2, CH_3	22.9, CH_3
15	27.3, CH_3	28.6, CH_3	26.2, CH_3	19.5, CH_3	23.6, CH_3	25.3, CH_3
1′	70.9, CH_2	67.6, CH_2	70.8, CH_2	70.6, CH_2	68.8, CH_2	69.6, CH_2
2′	54.0, C	56.1, C	57.1, C	61.1, C	60.6, C	57.0, C
3′	54.3, C	84.4, CH_2	161.0, C	55.6, C	56.2, C	70.3, C
4′	176.1, C	201.1, C	193.4, C	211.0, C	216.2, C	203.5, C
5′	139.3, C	51.1, C	54.3, C	52.1, C	50.6, C	51.6, C
6′	116.0, CH	145.2, CH	139.8, CH	145.8, CH	72.9, CH	146.2, CH
7′	44.2, CH	130.9, C	137.1, C	134.9, C	41.7, CH	139.5, C
8′	176.6, C	164.5, C	167.2, C	167.1, C	174.1, C	169.1, C
9′	11.2, CH_3	22.6, CH_3	26.6, CH_3	28.7, CH_3	62.8, CH_2	48.3, CH_2
10′	24.7, CH_3	27.9, CH_3	22.6, CH_3	16.7, CH_3	16.7, CH_3	20.0, CH_3
11′		61.4, CH_2	57.2, CH_3			
12′		14.3, CH_3				

[a]Recorded in $CDCl_3$. [b]Recorded in CD_3OD.

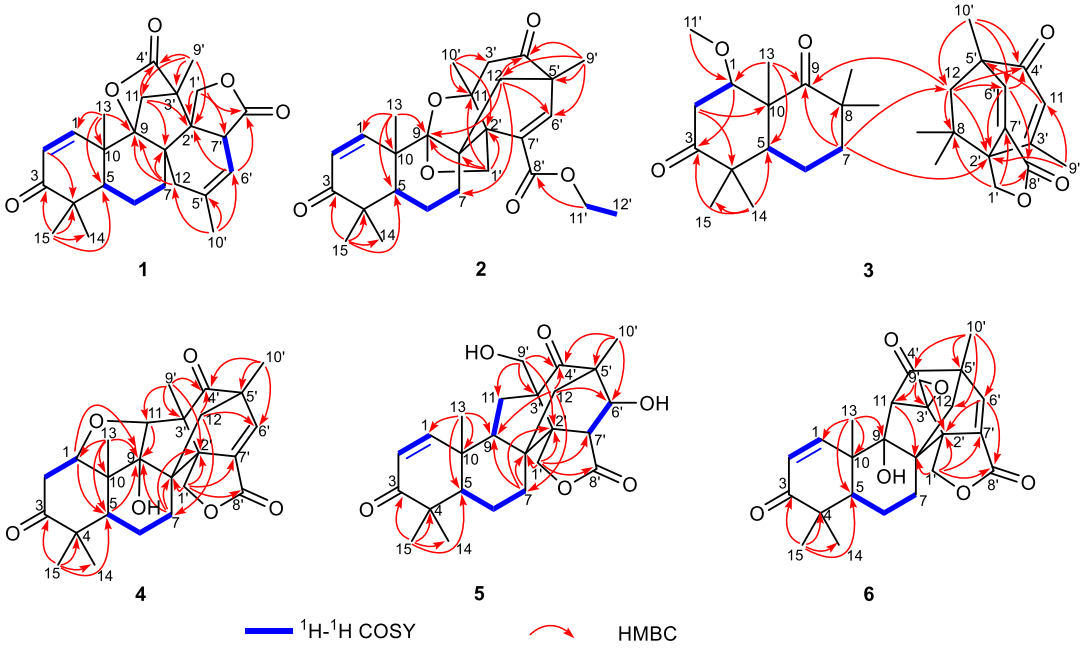

Figure 2. Selected ^{1}H−^{1}H COSY and HMBC correlations of compounds **1**−**6**.

overall ^{1}H and ^{13}C NMR data of **1** as well as the above elucidated rings A and B are similar to those of andiconin B (**9**),[11] except for the presence of a double bond and an ester carboxyl group (δ_C 176.1). HMBC correlations from H_2-11 to C-8 and C-2′, from H_3-9′ to C-11, C-2′, and C-3′, from H_3-10′ to C-12, C-5′, and C-6′, from H_2-12 to C-9, from H-6′ to C-2′ and C-8′, and from H-1′ to C-2′, C-7′, and C-8′ revealed that rings C, D, and F were constant with the presence of an additional $\Delta^{5',6'}$ double bond (δ_C 139.3 and 116.0) in ring D of **1**. Moreover, ring E of **9** was cleaved by Baeyer−Villiger oxidation and ring opening to generate an ester carboxyl group (δ_C 176.1) that replaced the ketone carbonyl (C-4′) in **9**. The connection of C-9 and C-4′, which formed a new lactone ring, was finally determined to satisfy the chemical shift of C-9 (δ_C 92.3) and the above

DOI: 10.1021/acs.joc.8b02830
J. Org. Chem. 2019, 84, 1534−1541

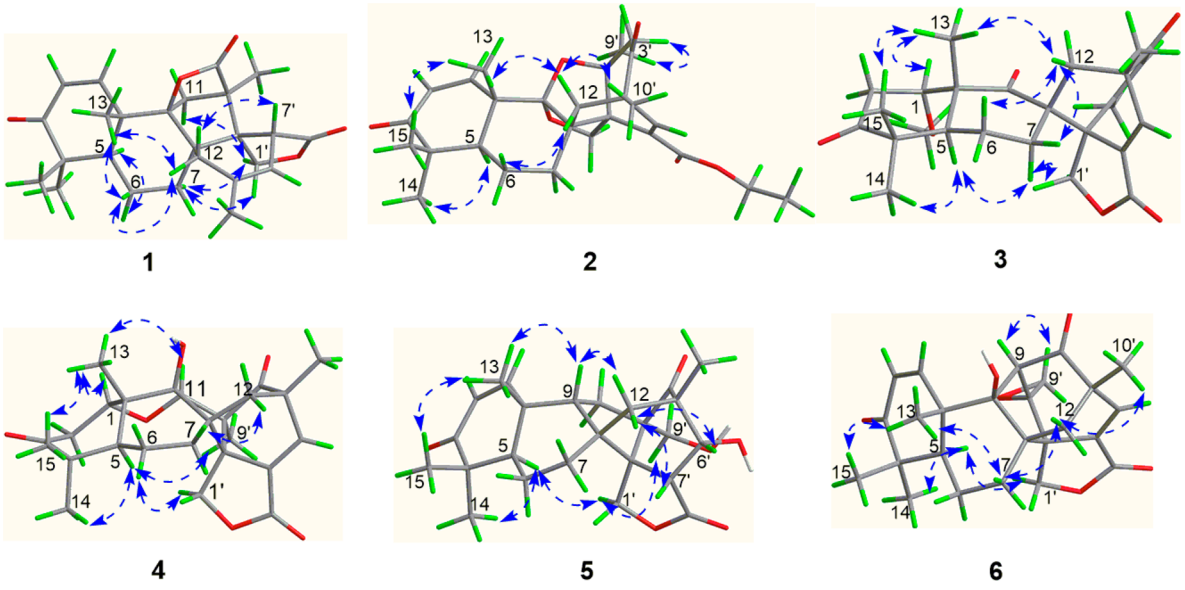

Figure 3. Selected NOESY correlations of compounds **1**−**6**.

elucidated degrees of unsaturation. Thus, the planar structure of **1** was determined.

The relative configuration of **1** was ascertained by the examination of its NOESY data (Figure 3). The NOESY correlations of H_3-13/H-6β and H-5/H-6α indicated that rings A and B were trans-fused, and the characteristic correlations of H_3-13/H-6β and H_2-12/H-6β suggested that the bond of C-8/C-12 should be β-oriented. Additionally, the NOESY correlation of H-7 with H_2-1′ disclosed the α-orientation of the C-2′/C-1′ bond. The interaction between H-1′b and H-11a revealed that the C-11 bridge should be α-oriented, and accordingly, the lactone group should be β-oriented, which determined the configurations of both C-9 and C-3′. Finally, the NOESY correlations of H-12a with H-7′ confirmed the orientation of H-7′ as shown.

Thus, the relative configuration of **1** was determined. To determine its absolute configuration, a time-dependent density functional theory (TDDFT) electronic circular dichroism (ECD) calculation was performed (Figure 4), and the almost identical calculated and experimental ECD curves confirmed the absolute configuration of **1** to be 5*R*,8*R*,9*R*,10*S*,2′*R*,3′*R*,7′*R*.

Compound **2** was isolated as a white powder. Its HRESIMS data disclosed a positive ion peak at m/z 455.2425, which corresponded to a molecular formula of $C_{27}H_{34}O_6$. The ^{1}H NMR data (Table 1) showed characteristic resonances of six methyl groups at δ_H 1.48 (s, H_3-10′), 1.33 (s, H_3-9′), 1.32 (t, J = 7.0 Hz, H_3-12′), 1.25 (s, H_3-13), 1.16 (s, H_3-14), and 1.11 (s, H_3-15), six methylenes including two oxygenated ones [δ_H 4.72 (1H, d, J = 9.1 Hz, H-1′), 4.06 (1H, d, J = 9.1 Hz, H-1′), and 4.21 (2H, q, J = 7.0 Hz, H-11′)], and three olefinic protons at δ_H 7.31 (d, J = 10.1 Hz, H-1), 5.91(d, J = 10.1 Hz, H-2), and 6.90 (s, H-6′). The ^{13}C NMR and DEPT data of **2** (Table 2) revealed 27 carbon resonances that were ascribed to six methyl groups, six methylene groups, four methine groups (including three olefinic ones), and eleven nonprotonated carbons (including two keto carbonyls, one ester carbonyl, and two oxygenated ones). The ^{1}H and ^{13}C NMR data of **2** closely resemble those of aspermerodione (**7**),[10] indicating that compound **2** shares a ring system similar to that of **7** with an unusual 2,6-dioxabicyclo[2.2.1]heptane moiety. The only difference was that the methoxyl group in **7** was replaced by an ethoxyl group in **2**, which could be deduced by the ^{1}H−^{1}H COSY cross-peak of H_2-11′/H_3-12′ and the HMBC correlation from H_2-11′ to C-8′ (δ_C 164.5) (Figure 2). Further 2D NMR spectra analyses confirmed its planar structure and relative configuration as shown in Figure 1. The absolute configuration of **2** was identical to that of **7** deduced by their closely similar experimental ECD spectra, which was further verified by the ECD calculation (Figure S1).

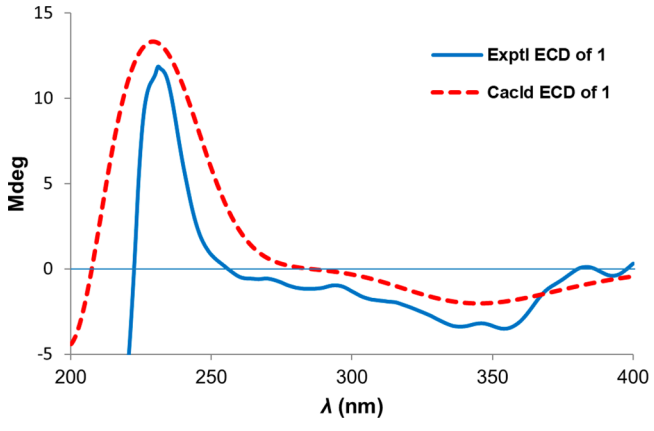

Figure 4. Experimental and calculated ECD spectra of **1**.

Compound **3** was isolated as colorless crystals (MeOH−CH_2Cl_2). Its HRESIMS data disclosed a positive ion peak at m/z 463.2092 ([M + Na]$^+$), which corresponded to a molecular formula of $C_{26}H_{32}O_6$. A comparison of the ^{13}C NMR and DEPT data between **3** (Table 2) and spiroaspertrione A (**11**),[11] the first meroterpenoid with a spiro[bicycle[3.2.2]nonane-2,1′-cyclohexane] carbocyclic skeleton, revealed high similarities, however, showing major differences in ring A. ^{1}H−^{1}H COSY correlation between H-1 (δ_H 3.95, t, J = 3.3 Hz) and H-2 (δ_H 2.69, t, J = 3.3 Hz) and the HMBC correlation from H_3-11′ (δ_H 3.28, s) to C-1 (δ_C 81.1) suggested that the Δ^1 double bond in **11** was replaced by an additional methoxyl group at C-1. Hence, the planar structure of **3** was established as shown in Figure 1. The relative configuration of **3** was partially ascertained by the

DOI: 10.1021/acs.joc.8b02830
J. Org. Chem. 2019, 84, 1534−1541

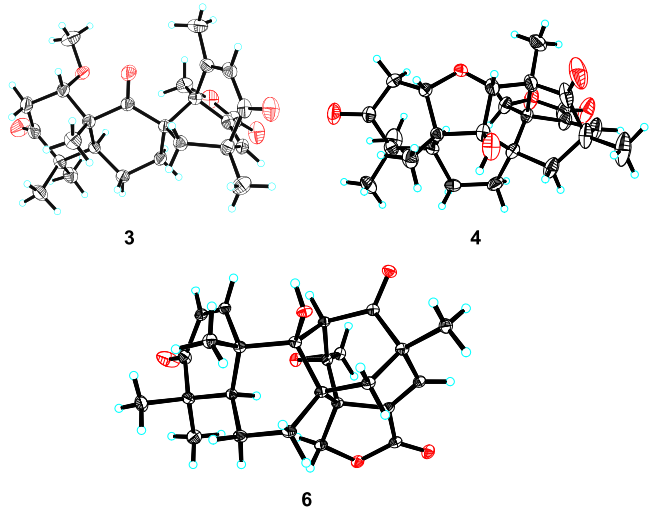

Figure 5. X-ray crystallographic structures of compounds **3**, **4**, and **6**.

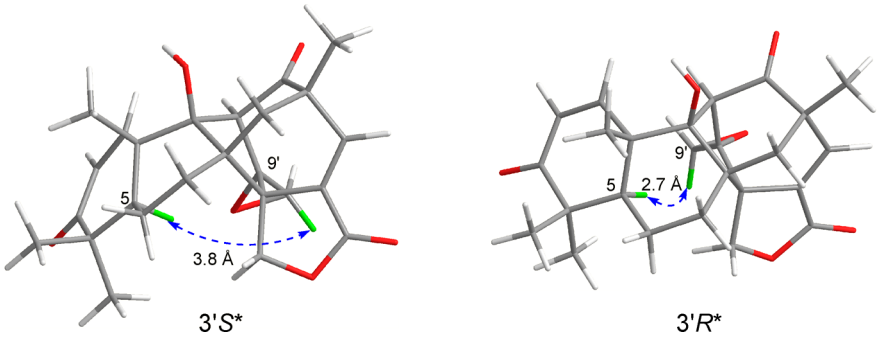

Figure 6. Two possible candidate structures (3′*S** and 3′*R**) of **6**.

examination of its NOESY spectrum (Figure 3). A single-crystal X-ray diffraction analysis of **3** was performed using Cu Kα radiation, which determined the absolute configuration of **3** as 1*S*,5*S*,8*R*,10*R*,2′*S*,5′*S* (Figure 5, CCDC 1830245).

Compound **4**, obtained as colorless crystals from MeOH, gave a HRESIMS ion peak at *m*/*z* 449.1906, corresponding to a molecular formula of $C_{25}H_{30}O_6$ with 11 degrees of unsaturation. The ^{1}H and ^{13}C NMR data of **4** (Tables 1 and 2) closely resembled those of andiconin C (**8**),[10] indicating that the two compounds shared an andiconin skeleton. The main difference is that the methine at C-9 in **8** is replaced by an oxygenated tertiary carbon (δ_C 88.8, C-9) in **4**, which was supported by the HMBC correlations (Figure 2) from H_3-13 to C-1, C-5, C-9, and C-10, from H-1 to C-5 and C-9, and from H-5 and H-11 to C-9. The planar structure of **4** was further confirmed by detailed analyses of its 2D NMR spectra. The NOESY spectrum (Figure 3) showed that the relative configuration of **4** is identical to that of **8**. A single-crystal X-ray diffraction analysis of **4** was performed by using Cu Kα radiation, which determined the absolute configuration of **4** as 1*S*,5*R*,8*R*,9*S*,10*R*,11*R*,2′*R*,3′*S*,5′*S* (Figure 5, CCDC 1866381).

Compound **5** was isolated as a white powder. Its HRESIMS data disclosed a molecular formula of $C_{25}H_{32}O_6$, which has one more oxygen atom than compound **9**.[11] Analyses of the NMR data (Tables 1 and 2) of **5** suggested the presence of four methyl groups, six methylenes including two oxygenated ones (δ_C 68.8, C-1′ and 62.8, C-9′), six methines including two olefinic carbons (δ_C 154.0 and 125.8), and nine nonprotonated carbons (including two ketone carbonyls and one ester carboxyl group). These data of **5** were closely similar to those of **9**, except that the methyl (C-9′) in **9** was replaced by an oxygenated methylenes (δ_C 62.8) in **5**. This was further verified by the HMBC correlations (Figure 2) from H_2-9′ (δ_H 3.89, d, *J* = 11.3 Hz and 3.71, d, *J* = 11.3 Hz) to C-2′ (δ_C 60.6), C-3′ (δ_C 56.2), C-4′ (δ_C 216.2), and C-11 (δ_C 34.8). The NOESY correlations of H_3-13/H_3-15, H-9/H-13/H_2-12, H_2-12/H-6′/H-7′, H-5/H_3-14/H_2-1′, and H_2-1′/H_2-9′ indicated that the relative configuration of **5** was the same as that of **9**. To determine its absolute configuration, the ECD spectra (Figure S2) of **5** were calculated. There is overall agreement between the experimental and predicted ECD curves of **5**. Therefore, the absolute configuration of **5** was established as 5*R*,8*S*,9*S*,10*R*,2′*R*,3′*R*,5′*S*,6′*R*,7′*R*.

Compound **6** was obtained as colorless crystals from a mixed solvent of CH_2Cl_2–MeOH (1:1). The molecular formula was determined as $C_{25}H_{28}O_6$ by HRESIMS and ^{13}C NMR data (Table 2). A detailed analysis of its ^{1}H NMR data (Table 1) demonstrated the presence of four methyl singlets at δ_H 1.36 (H_3-10′), 1.27 (H_3-13), 1.20 (H_3-14), and 1.13 (H_3-15), an oxygenated methylene at δ_H 4.52 (d, *J* = 9.6 Hz, H_2-1′) and 4.41 (d, *J* = 9.6 Hz, H_2-1′), and three olefinic protons at δ_H 6.91 (d, *J* = 10.3 Hz, H-1), 5.82 (d, *J* = 10.3 Hz, H-2), and 6.92 (s, H-6′). The ^{13}C NMR data, together with the DEPT spectrum, revealed the presence of 25 carbon resonances corresponding to four methyls, five methylenes, five methines (three olefinic ones), and eleven nonprotonated carbons (two carbonyls, one ester carbonyl, and one olefinic carbon). The presence of three carbonyls (δ_C 206.2, 203.5, and 169.1) and two double bonds

DOI: 10.1021/acs.joc.8b02830
J. Org. Chem. 2019, 84, 1534–1541

Scheme 1. Plausible Biosynthetic Pathway for Compound 1

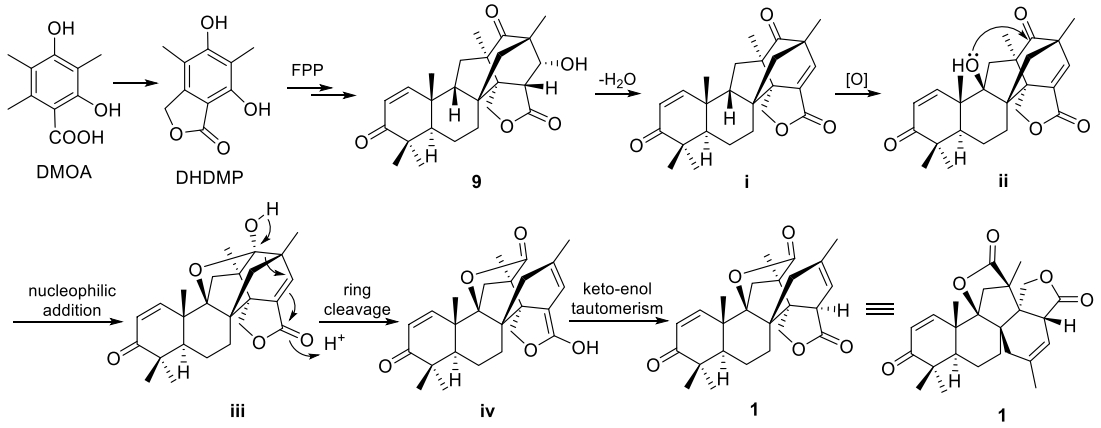

Table 3. Cytotoxic Activity of Compounds 1−6 (IC_{50} in μM)[a]

	HL-60	A-549	SMMC-7721	MCF-7	SW-480
1	>40	>40	>40	>40	>40
2	>40	>40	18.80 ± 0.23	>40	18.35 ± 0.53
3	>40	>40	>40	>40	>40
4	>40	11.33 ± 0.82	8.19 ± 0.39	>40	14.67 ± 1.12
5	>40	>40	>40	>40	>40
6	>40	>40	17.49 ± 0.59	>40	16.84 ± 1.08
DPP	6.28 ± 0.68	25.69 ± 1.60	20.72 ± 0.25	15.27 ± 0.51	19.55 ± 0.90

[a]DDP (cisplatin) was used as positive control. IC_{50} values are represented as the means ± SD based on three replicates.

(δ_C 155.5/126.1 and 146.2/139.5) accounted for five of twelve indexes of hydrogen deficiency, required for another seven rings in the structure. The ^{1}H and ^{13}C NMR data of **6** showed signals similar to those of emervaridone (**12**),[12] except for the replacement of the $\Delta^{3',9'}$ double bond by an epoxy group in **6**, suggested by the chemical shifts of C-3′ (δ_C 70.3) and C-9′ (δ_C 48.3) and H_2-9′ [δ_H 2.43 (overlapped) and 2.72 (d, J = 3.5 Hz)]. This conclusion was further supported by HMBC correlations (Figure 2) from H_2-9′ to C-2′ (δ_C 57.0), C-3′ (δ_C 70.3), and C-11 (δ_C 73.3). Thus, the planar structure of **6** was determined and further confirmed as shown in Figure 1.

The relative configuration of **6** was ascertained by the examination of its NOESY data, which was similar to that of **12** in displaying the NOESY correlations of H_3-13/H_3-15, H_3-14/H-5, H_3-13/H-7a, H-7a/H-12a, and H-5/H_2-1′. There are still two candidate structures with different configurations at C-3′, and the NOESY spectrum was further analyzed with the assistance of molecular modeling (Figure 6). As no NOESY correlation between H-5 and H-9′ was observed, the relative configuration of C-3′ was temporarily ascertained as *S**. Fortunately, after repeated recrystallization by various solvent systems, **6** furnished a high-quality crystal in CH_2Cl_2−MeOH (1:1) at room temperature, which was successfully subjected to a single-crystal X-ray diffraction experiment using Cu Kα radiation (Figure 5, CCDC 1830237), indicating the absolute configuration of **6** as 5*R*,8*R*,9*R*,10*S*,11*R*,2′*R*,3′*S*,5′*S*.

The known compounds were identified as aspermerodione (**7**),[10] andiconin C (**8**),[10] andiconin B (**9**),[11] emervaridone C (**10**),[8] spiroaspertrione A (**11**),[11] emervaridone (**12**),[12] emervaridone A (**13**),[8] and emervaridone B (**14**)[8] by comparing their ^{1}H and ^{13}C NMR spectroscopic data with literature values.

To the best of our knowledge, emeridone A (**1**) is a novel 3,5-demethylorsellinic acid-based meroterpenoid with a rare rigid tetracyclic 6/6/5/6 carbon ring system with two additional lactone rings. The biosynthetic origin for **1** was proposed as shown in Scheme 1. 3,5-Dimethylorsellinic acid and farnesyl pyrophosphate (FPP) served as biosynthetic precursors, accompanied by key cycloaddition and redox reactions to generate the key intermediate andiconin B (**9**).[6] Compound **9** subsequently participated in reactions of dehydration and oxidation to afford **ii**. Under the catalysis of acid, the intramolecular nucleophilic addition of 9-OH to the carbonyl C-4′ in **ii** provided a hemiketal intermediate **iii**. Afterward, the crucial cleavage and keto−enol tautomerism furnished the biosynthetic pathway of **1**. Compound **9** could also be transformed to other new compounds via reduction, dehydration, oxidation, and rearrangement reactions (Scheme S1, Supporting Information).[11,13]

Compounds **1**−**6** were evaluated for their cytotoxicity against five human cancer cell lines (HL-60, A-549, SMMC-7721, MCF-7, and SW-480) by the MTT method. The results (Table 3) showed that compounds **2**, **4**, and **6** exhibited moderate activities against SMMC-7721 cells, with IC_{50} values of 18.80, 8.19, and 17.49 μM, respectively. For the SW-480 cell line, compounds **2**, **4**, and **6** showed cytotoxicity with IC_{50} values of 18.35, 14.67, and 16.84 μM, respectively. Compound **4** also showed activity against A-549 cells with an IC_{50} of 11.33 μM.

In summary, emeridones A−F (**1**−**6**), six new 3,5-demethylorsellinic acid-based meroterpenoids, were isolated from *Emericella* sp. TJ29. Compound **1** represents the first meroterpenoid featuring a unique rigid 6/6/5/6 tetracyclic carbon ring system with two additional lactone rings formed by the carbon−carbon bond cleavage of **9**. The inhibitory effects on five human cancer cell lines were assessed in vitro. Compounds **2**, **4**, and **6** exhibited moderate cytotoxic activities.

DOI: 10.1021/acs.joc.8b02830
J. Org. Chem. 2019, 84, 1534−1541

EXPERIMENTAL SECTION

General Experimental Procedures. Optical rotations were determined with a PerkinElmer PE-341 polarimeter (PerkinElmer, Inc., Waltham, MA). UV spectra were measured by a PerkinElmer Lambda 35 spectrophotometer (PerkinElmer, Inc.). ECD data were obtained using a JASCO-810 spectrometer. IR spectra were recorded with a Bruker Vertex 70 FT-IR spectrophotometer (Bruker, Karlsruhe, Germany). NMR spectra were recorded on a Bruker AM-400 NMR spectrometer (Bruker, Karlsruhe, Germany). High-resolution electrospray ionization mass spectrometry (HRESIMS) data were acquired using a Bruker micrOTOF II spectrometer. Compounds were purified by a Dionex HPLC system semipreparative HPLC equipped with an Ultimate 3000 DAD detector (Thermo Fisher Scientific, Germany). Chemical shifts are expressed in ppm with reference to the $CDCl_3$ (δ_H 7.26/δ_C 77.0) and CD_3OD (δ_H 3.31/δ_C 49.0) signals. Single-crystal X-ray diffraction experiments were carried out with a Bruker APEX DUO diffractometer using graphite-monochromated Cu Kα radiation. Silica gel (80−120 mesh, 100−200 mesh, and 200−300 mesh, Qingdao Marine Chemical Inc., Qingdao, People's Republic of China), RP-C_{18} gel (50 μm, Merck Co. Ltd., Germany), and Sephadex LH-20 (GE Healthcare Bio-Sciences AB, Sweden) were used in the chromatography processes. Thin-layer chromatography (TLC) was performed with silica gel 60 F_{254} and RP-C_{18} F_{254} plates. Fractions were monitored by TLC, and spots were visualized by spraying heated silica gel plates with 10% H_2SO_4 in EtOH.

Fungus Material. The fungus *Emericella* sp.TJ29 was isolated from the root of the plant *Hypericum perforatum* collected from the Shennongjia areas of Hubei Province, China. The isolated fungus was identified based on morphology and a sequence analysis of the ITS region of the rDNA (GenBank accession No. KY 346979). A voucher fungal strain was deposited in the culture collection of Tongji Medical College, Huazhong University of Science and Technology.

Fermentation, Extraction, and Isolation. Mycelia of the fungus growing on malt extract agar were inoculated in a 250 mL Erlenmeyer flask containing 100 mL of malt extract broth medium [malt extract 2.0% (w/v), glucose 2.0% (w/v), and bacterial peptone 0.1% (w/v)] and cultured statically at room temperature for 21 days. Eighty liters in total of the whole culture broth was then filtered through a filter paper. The mycelia (6.0 kg of wet weight) were extracted with EtOAc (10 × 5 L). After the evaporation of the solvent, a dark brown solid (200.0 g) was obtained, which was extracted with ethyl acetate (5 × 5 L). The ethyl acetate extract was evaporated under reduced pressure, leaving a brown viscous residue (89.0 g) that was chromatographed over silica gel (80−120 mesh) and eluted with a gradient system of petroleum ether−EtOAc (100:0 → 0:100, v/v) to give five fractions (Fr.1−Fr.5).

Fr.2 (9.4 g) was further fractionated on a silica gel column chromatograph (CC) eluted with CH_2Cl_2−MeOH (80:1−0:1) to obtain four major fractions (Fr.2.1−Fr.2.4). Fr.2.3 (3.7 g) was chromatographed using Sephadex LH-20 (MeOH) to give four fractions. Fr.2.3.2 (50.2 mg) and Fr.2.3.3 (38.2 mg) were purified by semipreparative HPLC (MeOH−H_2O, 60:40, v/v) to yield **2** (19.8 mg) and **7** (12.4 mg), respectively.

Fr.3 (28.4 g) was further separated by Sephadex LH-20 (CH_2Cl_2−MeOH, 1:1, v/v) followed by reversed-phase ODS CC [23.6 g, MeOH−H_2O (20, 40, 60, 80, 100%)] to afford five fractions (Fr.3.1−Fr.3.5). Fr.3.2 (3.3 g) was further fractionated on a silica gel CC eluted with CH_2Cl_2−MeOH (80:1−0:1) to obtain seven major fractions (Fr.3.2.1−Fr.3.2.7) based on TLC analysis. Fr.3.2.3 (142.0 mg) was purified by semipreparative HPLC (MeOH−H_2O,68:32, v/v) to afford compounds **6** (10.0 mg) and **11** (36.0 mg). Fr.3.2.4 (162.1 mg) was purified by semipreparative HPLC (acetonitrile−H_2O, 53:47, v/v) to yield **4** (11.0 mg), **9** (28.0 mg), and **12** (20.0 mg). Fr.3.2.5 (90.6 mg) was purified by semipreparative HPLC (acetonitrile−H_2O, 55:45, v/v) to afford compounds **13** (39.0 mg) and **14** (35.1 mg). Fr.3.3 (2.1 g) was further fractionated on a silica gel CC eluted with CH_2Cl_2−MeOH (20:1−0:1) to obtain six major fractions (Fr.3.3.1−Fr.3.3.6). Fr.3.3.3 (62.8 mg) was purified by semipreparative HPLC (MeOH−H_2O, 65:35, v/v) to afford compounds **3** (8.7 mg), **8** (29.0 mg), and **10** (8.3 mg). Fr.3.3.4 (45.0 mg) was purified by semipreparative HPLC (acetonitrile−H_2O, 45:55, v/v) to afford compounds **1** (8.2 mg).

Fr.4 (5.6 g) was further fractionated on a silica gel CC eluted with ether−EtOAc (10:1−1:1) to obtain six major fractions (Fr.4.1−Fr.4.6) based on TLC analysis. Fr.4.3 (0.7 g) was chromatographed using Sephadex LH-20 (MeOH) to give three fractions. Fr.4.3.2 (50.2 mg) was purified by semipreparative HPLC (MeOH−H_2O, 52:48, v/v) to yield **5** (8.5 mg).

Emeridone A (**1**): $C_{25}H_{30}O_5$; white power; $[\alpha]^{25}_D$ −17.1 (*c* 0.28, CH_2Cl_2); UV (CH_2Cl_2) λ_{max} (log ε) = 229 (3.32) nm; IR (KBr) ν_{max} = 3440, 2965, 1781, 1666, 1461, 1384, and 1258 cm^{-1}; CD (CH_2Cl_2) λ_{max} ($\Delta\varepsilon$) = 232 (+2.2), 337 (−0.6) nm; for ^1H and ^{13}C NMR data see Tables 1 and 2; HRMS (ESI-TOF) *m*/*z*: $[M + Na]^+$ Calcd for $C_{25}H_{30}O_5Na$, 433.1991; found 433.2002.

Emeridone B (**2**): $C_{27}H_{34}O_6$; white power; $[\alpha]^{25}_D$ −20.7 (*c* 0.09, MeOH); UV (CH_2Cl_2) λ_{max} (log ε) = 231 (3.79) nm; IR (KBr) ν_{max} = 3431, 2973, 2935, 1771, 1666, 1457,1380, and 1263 cm^{-1}; CD (CH_2Cl_2) λ_{max} ($\Delta\varepsilon$) = 216 (+3.1), 294 (−2.4) nm; for ^1H and ^{13}C NMR data, see Tables 1 and 2; HRMS (ESI-TOF) *m*/*z*: $[M + H]^+$ Calcd for $C_{27}H_{35}O_6$, 455.2434; found 455.2425.

Emeridone C (**3**): $C_{26}H_{32}O_6$; colorless crystals; mp 198−199 °C; $[\alpha]^{25}_D$ −77.9 (*c* 0.19, MeOH); UV (CH_2Cl_2) λ_{max} (log ε) = 229 (3.66) nm; IR (KBr) ν_{max} = 3434, 2934, 1764, 1707, 1660, 1454, 1378, and 1240 cm^{-1}; CD (CH_2Cl_2) λ_{max} ($\Delta\varepsilon$) = 232 (−4.2), 277 (+1.9) nm; for ^1H and ^{13}C NMR data see Tables 1 and 2; HRMS (ESI-TOF) *m*/*z*: $[M + Na]^+$ Calcd for $C_{26}H_{32}O_6Na$, 463.2097; found 463.2092.

Emeridone D (**4**): $C_{25}H_{30}O_6$; colorless crystals; mp 201−202 °C; $[\alpha]^{25}_D$ −21.8 (*c* 0.11, CH_2Cl_2); UV (CH_2Cl_2) λ_{max} (log ε) = 229 (3.28) and 248 (3.11) nm; IR (KBr) ν_{max} = 3442, 2972, 2931, 1723, 1663, 1458, 1381, and 1259 cm^{-1}; CD (CH_2Cl_2) λ_{max} ($\Delta\varepsilon$) = 211 (+3.9), 309 (−2.1) nm; for ^1H NMR and ^{13}C NMR data, see Tables 1 and 2; HRMS (ESI-TOF) *m*/*z*: $[M + H]^+$ Calcd for $C_{25}H_{31}O_6$, 427.2121; found 427.2115.

Emeridone E (**5**): $C_{25}H_{32}O_6$; white power; $[\alpha]^{25}_D$ −17.5 (*c* 0.08, MeOH); UV (CH_2Cl_2) λ_{max} (log ε) = 204(3.78) and 222(3.71) nm; IR (KBr) ν_{max} = 3427, 2968, 2931, 2886, 1770, 1720, 1670, and 1462 cm^{-1}; CD (CH_2Cl_2) λ_{max} ($\Delta\varepsilon$) = 296 (−2.9), 330 (+0.8) nm; for ^1H NMR and ^{13}C NMR data, see Tables 1 and 2; HRMS (ESI-TOF) *m*/*z*: $[M + Na]^+$ Calcd for $C_{25}H_{32}O_6Na$, 451.2097; found 451.2093.

Emeridone F (**6**): $C_{25}H_{28}O_6$; colorless crystals; mp 200−201 °C; $[\alpha]^{25}_D$ −53.1(*c* 0.65, CH_2Cl_2); UV (CH_2Cl_2) λ_{max} (log ε) = 229 (3.80) nm; IR (KBr) ν_{max} = 3440, 2972, 1760, 1723, 1662, 1460, 1381, and 1257 cm^{-1}; CD (CH_2Cl_2) λ_{max} ($\Delta\varepsilon$) = 218 (+2.8), 293 (−2.2) nm; for ^1H and ^{13}C NMR data, see Tables 1 and 2; HRMS (ESI-TOF) *m*/*z*: $[M + Na]^+$ Calcd for $C_{25}H_{28}O_6Na$, 447.1784; found 447.1783.

The Crystallographic data (excluding structure factor tables) for the reported structures have been deposited with the Cambridge Crystallographic Data Center (CCDC) as supplementary publication nos. CCDC 1830245 for **3**, CCDC 1866381 for **4**, and CCDC 1830237 for **6**. Copies of the data can be obtained free of charge from the CCDC, 12 Union Road, Cambridge CB2 1EZ, UK [fax: + 44(0)1223 336 033; e-mail: deposit@ccdc.cam.ac.uk).

Crystallographic data for emeridone C (**3**): $C_{26}H_{32}O_6$, *M* = 440.51, *a* = 8.9473(8) Å, *b* = 13.6391(12) Å, *c* = 9.5262(8) Å, α = 90°, β = 105.518(5)°, γ = 90°, *V* = 1120.13(17) Å^3, *T* = 296(2) K, space group $P2_1$, *Z* = 2, μ(Cu Kα) = 0.747 mm^{-1}, 11816 reflections measured, 3805 independent reflections (R_{int} = 0.0344). The final R_1 values were 0.0332 ($I > 2\sigma(I)$). The final $wR(F^2)$ values were 0.0876 ($I > 2\sigma(I)$). The final R_1 values were 0.0332 (all data). The final $wR(F^2)$ values were 0.0876 (all data). The goodness of fit on F^2 was 1.057. Flack parameter = 0.09(5).

Crystallographic data for emeridone D (**4**): $C_{25}H_{30}O_6$, *M* = 424.18, *a* = 25.0931(2) Å, *b* = 23.3230(2) Å, *c* = 7.67857(7) Å, α = 90°, β = 90°, γ = 90°, *V* = 4493.86(7) Å^3, *T* = 295.41(10) K, space group $P2_12_12$, *Z* = 8, μ(Cu Kα) = 0.742 mm^{-1}, 21565 reflections measured, 7885 independent reflections (R_{int} = 0.0244). The final R_1 values were 0.0590 ($I > 2\sigma(I)$). The final $wR(F^2)$ values were 0.1739 ($I > 2\sigma(I)$). The final R_1 values were 0.0625 (all data). The final $wR(F^2)$ values were 0.1784 (all data). The goodness of fit on F^2 was 1.055. Flack parameter = 0.06(7).

DOI: 10.1021/acs.joc.8b02830
J. Org. Chem. 2019, 84, 1534−1541

Crystallographic data for emeridone F (**6**): $C_{25}H_{28}O_6$, M = 424.18, a = 7.9644(10) Å, b = 10.5027(10) Å, c = 12.5674(2) Å, α = 91.4630(10)°, β = 90.4070(10)°, γ = 100.6940(10)°, V = 1032.56(2) Å^3, T = 150(10) K, space group $P1$, Z = 2, μ(Cu Kα) = 0.822 mm^{-1}, 35184 reflections measured, 7885 independent reflections (R_{int} = 0.0270). The final R_1 values were 0.0311 ($I > 2\sigma(I)$). The final $wR(F^2)$ values were 0.0820 ($I > 2\sigma(I)$). The final R_1 values were 0.0312 (all data). The final $wR(F^2)$ values were 0.0820 (all data). The goodness of fit on F^2 was 1.062. Flack parameter = 0.01(6).

ECD Calculations. The theoretical calculations of new compounds **1**, **2**, and **5** were performed using Gaussian 09. Conformational analysis was initially conducted by using Maestro in Schrodinger 2010 conformational searching, together with the OPLS_2005 molecular mechanics methods. The optimized conformation geometries and thermodynamic parameters of all conformations were provided. The OPLS_2005 conformers were optimized at the B3LYP/6-311G(d) level. The theoretical calculation of ECD was performed using TDDFT at the B3LYP/6-311++G** level in CH_2Cl_2 with the PCM model. The calculated ECD curves were generated using SpecDis 1.51. R_{vel}.

In Vitro Cytotoxicity. Five human cancer cell lines HL-60, SMMC-7721, A549, MCF-7, and SW-480 were used in the cytotoxic activity assay, as described in our previous report.[14]

■ ASSOCIATED CONTENT

Supporting Information

The Supporting Information is available free of charge on the ACS Publications website at DOI: 10.1021/acs.joc.8b02830.

ECD calculation details of **1**, **2**, and **5** and results for **2** and **5**, X-ray crystallographic data of **3**, **4**, and **6**, hypothetical biosynthetic pathway of **2**−**14**, NMR, HRESIMS, UV, and IR spectra of **1**−**6** (PDF)

X-ray crystallographic data of **3** (CIF)

X-ray crystallographic data of **4** (CIF)

X-ray crystallographic data of **6** (CIF)

■ AUTHOR INFORMATION

Corresponding Authors

*E-mail: zhangyh@mails.tjmu.edu.cn.

*E-mail: zhuhucheng@hust.edu.cn.

ORCID

Junjun Liu: 0000-0001-9953-8633

Yonghui Zhang: 0000-0002-7222-2142

Author Contributions

‖These authors contributed equally to this work.

Notes

The authors declare no competing financial interest.

■ ACKNOWLEDGMENTS

This work was financially supported by the Program for Changjiang Scholars of the Ministry of Education of the People's Republic of China (no. T2016088), the National Natural Science Foundation for Distinguished Young Scholars (no. 81725021), the National Science and Technology Project of China (2018ZX09201001-001-003), Innovative Research Groups of the National Natural Science Foundation of China (81721005), the National Natural Science Foundation of China (no. 81803387), the Academic Frontier Youth Team of HUST, and the Integrated Innovative Team for Major Human Diseases Program of Tongji Medical College (HUST). We thank the Analytical and Testing Center at Huazhong University of Science and Technology for assistance in the acquisition of the ECD, UV, and IR spectra.

■ REFERENCES

(1) Hou, J. Q.; Guo, C.; Zhao, J. J.; Dong, Y. Y.; Hu, X. L.; He, Q. W.; Zhang, B. B.; Yan, M.; Wang, H. Anti-Inflammatory Meroterpenoids from *Baeckea Frutescens*. *J. Nat. Prod.* **2017**, *80*, 2204−2214.

(2) Zhou, H.; Sun, X.; Li, N.; Che, Q.; Zhu, T.; Gu, Q.; Li, D. Isoindolone-Containing Meroperpenoids from the Endophytic Fungus *Emericella Nidulans* HDN12−249. *Org. Lett.* **2016**, *18*, 4670−4673.

(3) Li, Y.; Niu, S.; Sun, B.; Liu, S.; Liu, X.; Che, Y. Cytosporolides A−C, Antimicrobial Meroterpenoids with a Unique Peroxylactone Skeleton from *Cytospora* sp. *Org. Lett.* **2010**, *12*, 3144−3147.

(4) Qi, C.; Bao, J.; Wang, J.; Zhu, H.; Xue, Y.; Wang, X.; Li, H.; Sun, W.; Gao, W.; Lai, Y.; Chen, J.-G.; Zhang, Y. Asperterpenes A and B, Two Unprecedented meroterpenoids from *Aspergillus Terreus* with Bace1 inhibitory activities. *Chemi. Sci.* **2016**, *7*, 6563−6572.

(5) Lo, H. C.; Entwistle, R.; Guo, C.-J.; Ahuja, M.; Szewczyk, E.; Hung, J.-H.; Chiang, Y.-M.; Oakley, B. R.; Wang, C. C. Two Separate Gene Clusters Encode the Biosynthetic Pathway for the Meroterpenoids Austinol and Dehydroaustinol in *Aspergillus Nidulans*. *J. Am. Chem. Soc.* **2012**, *134*, 4709−4720.

(6) Matsuda, Y.; Abe, I. Biosynthesis of Fungal Meroterpenoids. *Nat. Prod. Rep.* **2016**, *33*, 26−53.

(7) Qi, C.; Liu, M.; Zhou, Q.; Gao, W.; Chen, C.; Lai, Y.; Hu, Z.; Xue, Y.; Zhang, J.; Li, D.; Li, X.-N.; Zhang, Q.; Wang, J.; Zhu, H.; Zhang, Y. BACE1 Inhibitory Meroterpenoids from *Aspergillus Terreus*. *J. Nat. Prod.* **2018**, *81*, 1937−1945.

(8) He, Y.; Hu, Z.; Li, Q.; Huang, J.; Li, X. N.; Zhu, H.; Liu, J.; Wang, J.; Xue, Y.; Zhang, Y. Bioassay-Guided Isolation of Antibacterial Metabolites from *Emericella* sp. TJ29. *J. Nat. Prod.* **2017**, *80*, 2399−2405.

(9) Grothe, E.; Moo-Young, M.; Chisti, Y. Fermentation Optimization for the production of Poly(β-Hydroxybutyric acid) microbial thermoplastic. *Enzyme Microb. Technol.* **1999**, *25*, 132−141.

(10) Qiao, Y.; Zhang, X.; He, Y.; Sun, W.; Feng, W.; Liu, J.; Hu, Z.; Xu, Q.; Zhu, H.; Zhang, J.; Luo, Z.; Wang, J.; Xue, Y.; Zhang, Y. Aspermerodione, a Novel Fungal metabolite with an unusual 2,6-Dioxabicyclo[2.2.1]heptane skeleton, as an inhibitor of penicillin-binding Protein 2a. *Sci. Rep.* **2018**, *8*, 5454.

(11) He, Y.; Hu, Z.; Sun, W.; Li, Q.; Li, X. N.; Zhu, H.; Huang, J.; Liu, J.; Wang, J.; Xue, Y.; Zhang, Y. Spiroaspertrione A, a Bridged Spirocyclic Meroterpenoid, as a Potent Potentiator of Oxacillin against Methicillin-Resistant Staphylococcus Aureus from *Aspergillus* sp. TJ23. *J. Org. Chem.* **2017**, *82*, 3125−3131.

(12) Liangsakul, J.; Pornpakakul, S.; Sangvichien, E.; Muangsin, N.; Sihanonth, P. Emervaridione and Varioxiranediol, two new metabolites from the endophytic Fungus. *Tetrahedron Lett.* **2011**, *52*, 6427−6430.

(13) Matsuda, Y.; Wakimoto, T.; Mori, T.; Awakawa, T.; Abe, I. Complete Biosynthetic Pathway of Anditomin: Nature's Sophisticated Synthetic Route to a Complex Fungal Meroterpenoid. *J. Am. Chem. Soc.* **2014**, *136*, 15326−15336.

(14) Zhu, H.; Chen, C.; Yang, J.; Li, X.-N.; Liu, J.; Sun, B.; Huang, S. X.; Li, D.; Yao, G.; Luo, Z.; Li, Y.; Zhang, J.; Xue, Y.; Zhang, Y. Bioactive Acylphloroglucinols with Adamantyl Skeleton from *Hypericum Sampsonii*. *Org. Lett.* **2014**, *16*, 6322−6325.

DOI: 10.1021/acs.joc.8b02830
J. Org. Chem. 2019, 84, 1534−1541